Supplement of Atmos. Chem. Phys., 21, 13537–13551, 2021
https://doi.org/10.5194/acp-21-13537-2021-supplement

Supplement of

Reactions of NO_3 with aromatic aldehydes: gas-phase kinetics and insights into the mechanism of the reaction

Yangang Ren et al.

Correspondence to: Abdelwahid Mellouki (mellouki@cnrs-orleans.fr) and A. R. Ravishankara (a.r.ravishankara@colostate.edu)

1. Error analysis

The quoted uncertainties in $\frac{k}{k_{ref}}$ ratios were estimated as follows: (1) The standard deviations of the least-squares fits of plots of $\ln\frac{[aromatic\ aldehyde]_0}{[aromatic\ aldehyde]_t} - k_d * t$ against $\ln\frac{[reference]_0}{[reference]_t} - k_d * t$ were calculated and twice this value was used; (2) the weighted average and error of repeated sampling was calculated using Eq.S2 and Eq.S3; (3) the total error in $\frac{k}{k_{ref}}$ was obtained by multiplying the computed error by factor of 2.9 (according to the Student *t*-distribution contribution) to account for the limited number of measurements.

The overall uncertainties for rate coefficients using the following propagation of uncertainty:

$$\frac{k}{k_{\mathrm{ref}}} k_{\mathrm{ref}} \sqrt{\left[\frac{\sigma_{k_{\mathrm{ref}}}}{k_{\mathrm{ref}}}\right]^2 + \left[\frac{\sigma_{\frac{k}{k_{\mathrm{ref}}}}}{\frac{k}{k_{\mathrm{ref}}}}\right]^2} \qquad \text{Eq.S1}$$

The weighted average is given by:

$$k_{average}=(w_1k_1 + w_2k_2 + \ldots)/(w_1+w_2+\ldots), \text{ where } w=1/\sigma^2, \text{ etc.} \qquad \text{Eq.S2}$$

The error in this average, $\sigma_{average}$, is given by:

$$\sigma_{av}= \left(\frac{1}{\sigma_1^2} + \frac{1}{\sigma_2^2} + \ldots\right)^{-0.5} \qquad \text{Eq.S3}$$

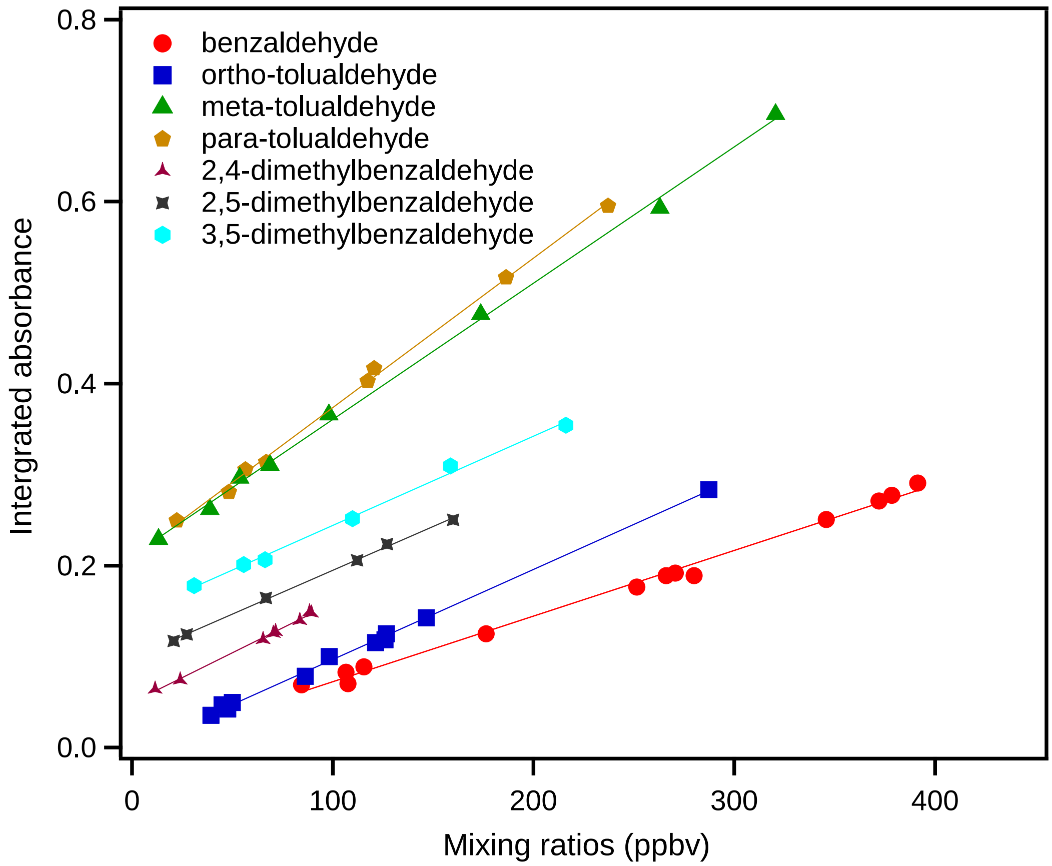

Figure S1. Calibration curve for studied aromatic aldehydes. Plots of the integrated absorbance (shown in Table S1) as a function of the mixing ratio in the chamber determined by manometric measurements for the various aldehydes noted in the legend. The data were fitted using a linear least-squares algorithm, assuming that the intercepts are zero. For the sake of clarity, the plots of 2,4-DMBA, 2,5-DMBA, 3,5-DMBA, M-TA and P-TA are displaced vertically by 0.05, 0.1, 0.15, 0.2 and 0.2, respectively.

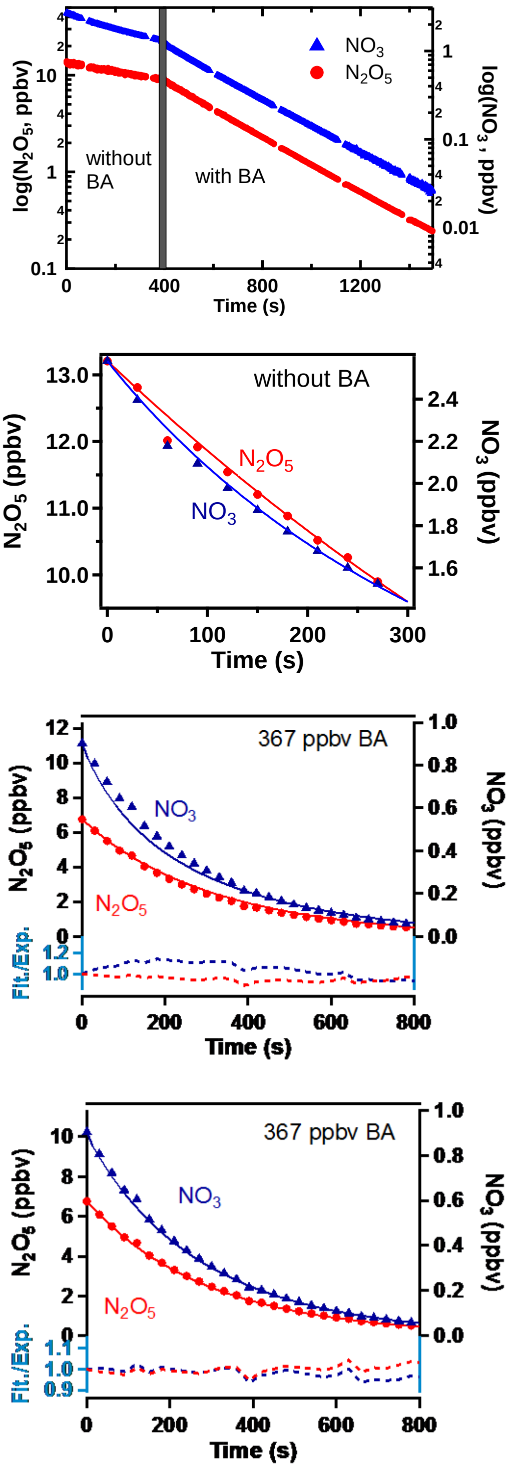

Figure S2 Observed (data points) and simulated (lines) profiles of N_2O_5 and NO_3 as functions of reaction time for the reaction of NO_3 with benzaldehyde. The dashed lines in the bottom panels show the ratio between simulated and observed values (Fit./Exp.). Mixing ratios of benzaldehyde are shown in each panel. The first panel is the time profile on a log scale. The data in the second panel was used to determine the wall loss of N_2O_5 and NO_3. The simulations in the third panel did not include subsequent reactions of the products of the NO_3 reaction. The data in the bottom panel included all possible subsequent reactions (shown in Table S4). It shows that the subsequent reactions do contribute to the long-term profiles.

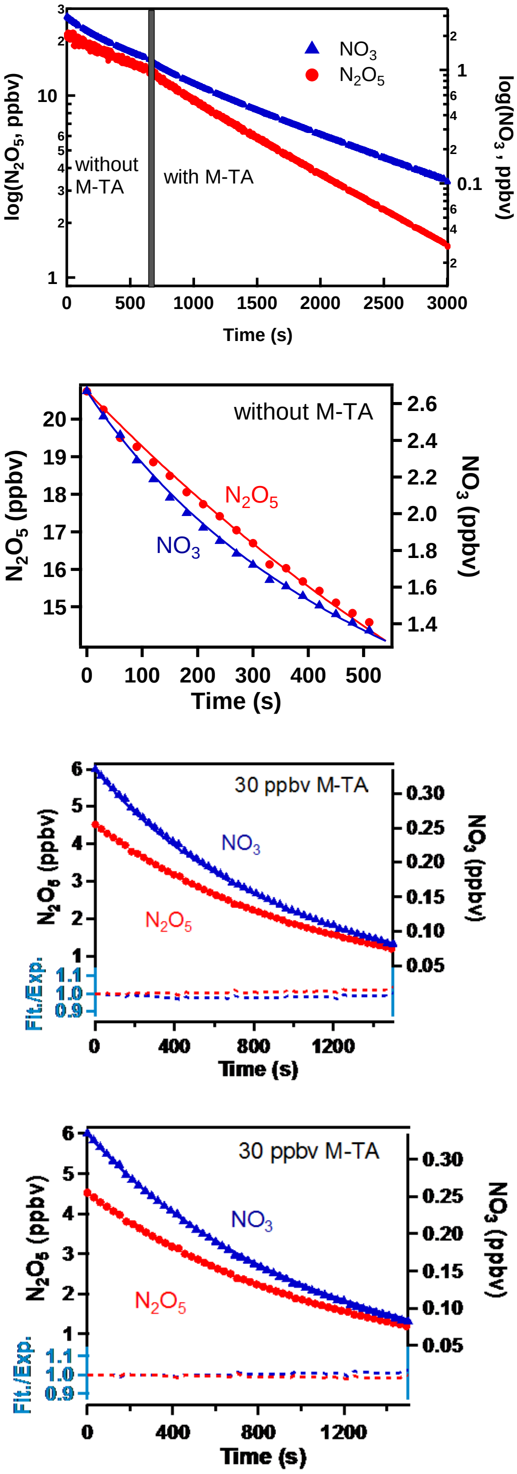

Figure S3 Observed (data points) and simulated (lines) profiles of N_2O_5 and NO_3 as functions of reaction time for the reaction of NO_3 with m-tolualdehyde. The dash lines in the bottom panels show the ratio between simulated and observed values (Fit./Exp.). Mixing ratios of benzaldehyde are shown in each panel. The first panel is the time profile on a log scale. The data in the second panel was used to determine the wall loss of N_2O_5 and NO_3. The simulations in the third panel did not include subsequent reactions of the products of the NO_3 reaction. The data in the bottom panel included all possible subsequent reactions (shown in Table S4). It shows that the subsequent reactions do contribute to the long-term profiles.

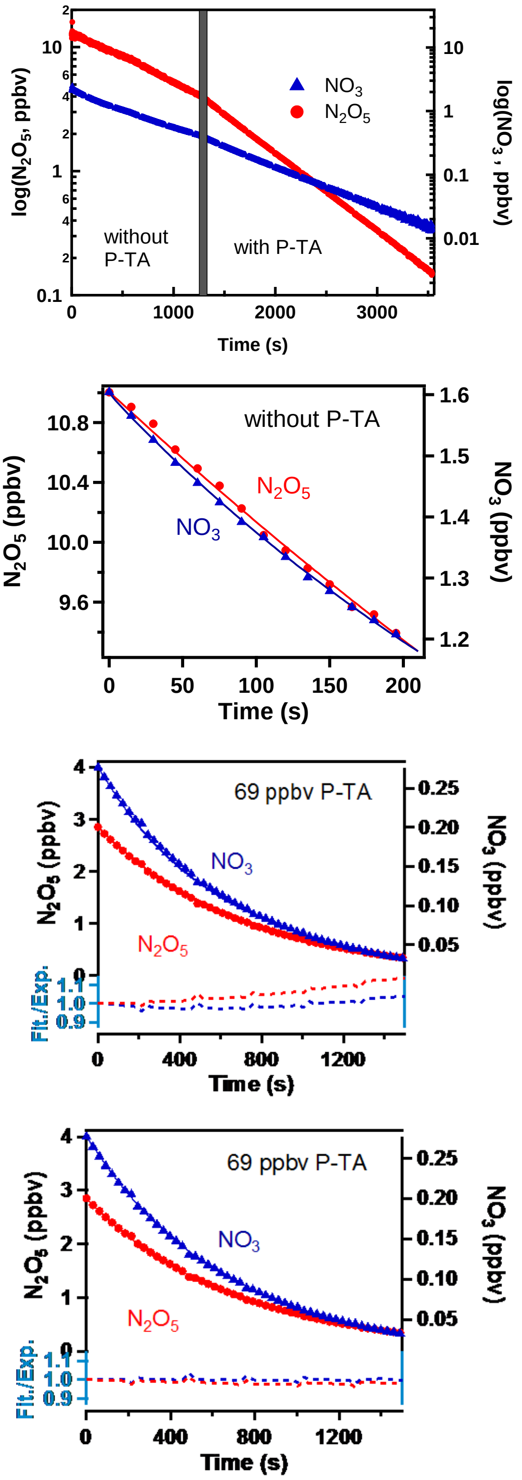

Figure S4 Observed (data points) and simulated (lines) profiles of N_2O_5 and NO_3 as functions of reaction time for the reaction of NO_3 with p-tolualdehyde. The dashed lines in the bottom two panels show the ratio between simulated and observed values (Fit./Exp.). Mixing ratios of benzaldehyde are shown in each panel. The first panel is the time profile on a log scale. The data in the second panel was used to determine the wall loss of N_2O_5 and NO_3. The simulations in the third panel did not include subsequent reactions of the products of the NO_3 reaction. The data in the bottom panel included all possible subsequent reactions (shown in Table S4). It shows that the subsequent reactions do contribute to the long-term profiles.

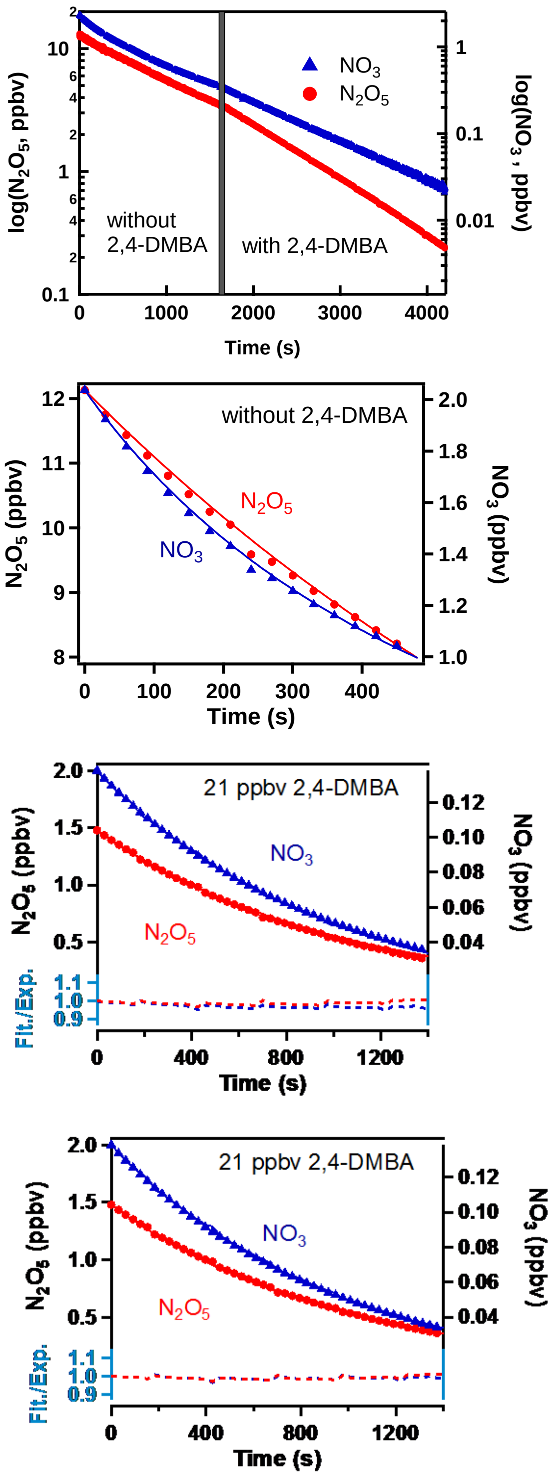

Figure S5 Observed (data points) and simulated (lines) profiles of N_2O_5 and NO_3 as functions of reaction time for the reaction of NO_3 with 2,4-dimethyl benzene. The dashed lines in the bottom two panels show the ratio between simulated and observed values (Fit./Exp.). Mixing ratios of benzaldehyde are shown in each panel. The first panel is the time profile on a log scale. The data in the second panel was used to determine the wall loss of N_2O_5 and NO_3. The simulations in the third panel did not include subsequent reactions of the products of the NO_3 reaction. The data in the bottom panel included all possible subsequent reactions (shown in Table S4). It shows that the subsequent reactions do contribute to the long-term profiles.

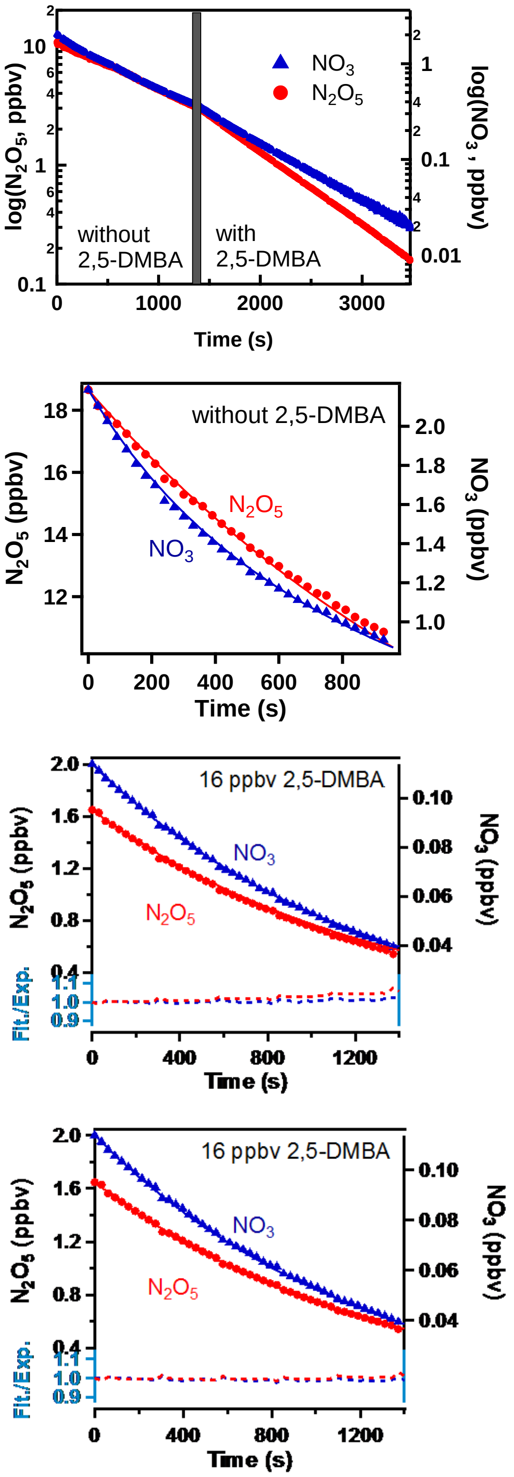

Figure S6 Observed (data points) and simulated (lines) profiles of N_2O_5 and NO_3 as functions of reaction time for the reaction of NO_3 with 2,5-dimethyl benzene. The dashed lines in the bottom two panels show the ratio between simulated and observed values (Fit./Exp.). Mixing ratios of benzaldehyde are shown in each panel. The first panel is the time profile on a log scale. The data in the second panel was used to determine the wall loss of N_2O_5 and NO_3. The simulations in the third panel did not include subsequent reactions of the products of the NO_3 reaction. The data in the bottom panel included all possible subsequent reactions (shown in Table S4). It shows that the subsequent reactions do contribute to the long-term profiles.

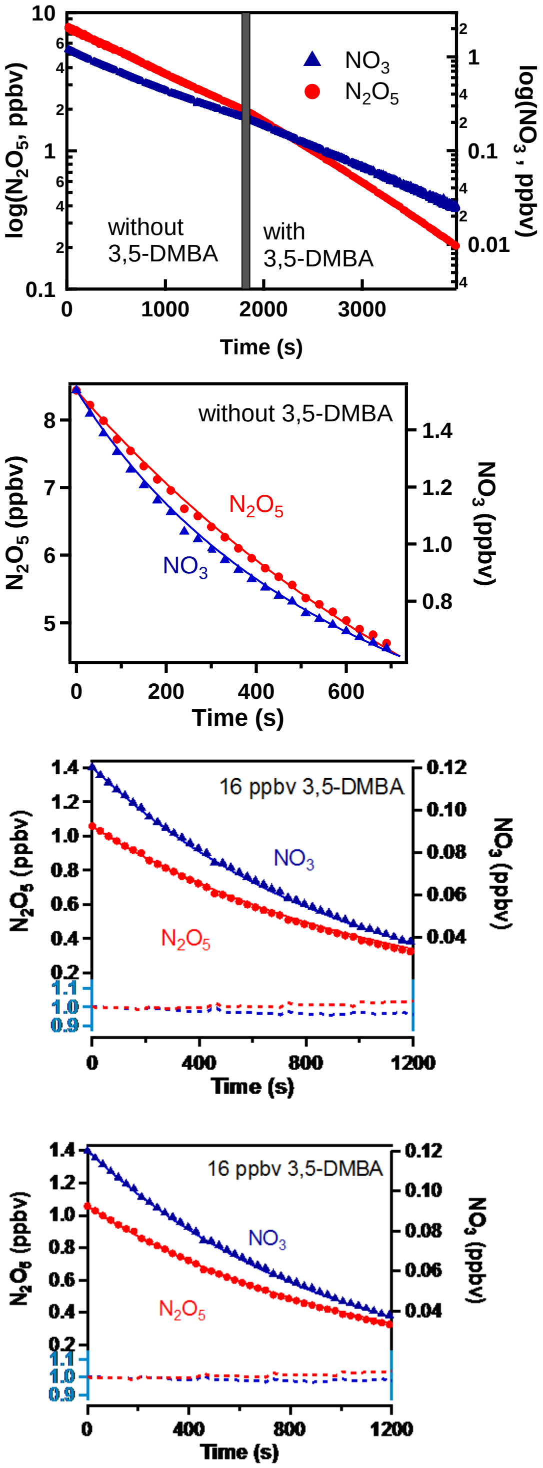

Figure S7 Observed (data points) and simulated (lines) profiles of N_2O_5 and NO_3 as functions of reaction time for the reaction of NO_3 with 3,5-dimethyl benzene. The dashed lines in the bottom two panels show the ratio between simulated and observed values (Fit./Exp.). Mixing ratios of benzaldehyde are shown in each panel. The first panel is the time profile on a log scale. The data in the second panel was used to determine the wall loss of N_2O_5 and NO_3. The simulations in the third panel did not include subsequent reactions of the products of the NO_3 reaction. The data in the bottom panel included all possible subsequent reactions (shown in Table S4). It shows that the subsequent reactions do contribute to the long-term profiles.

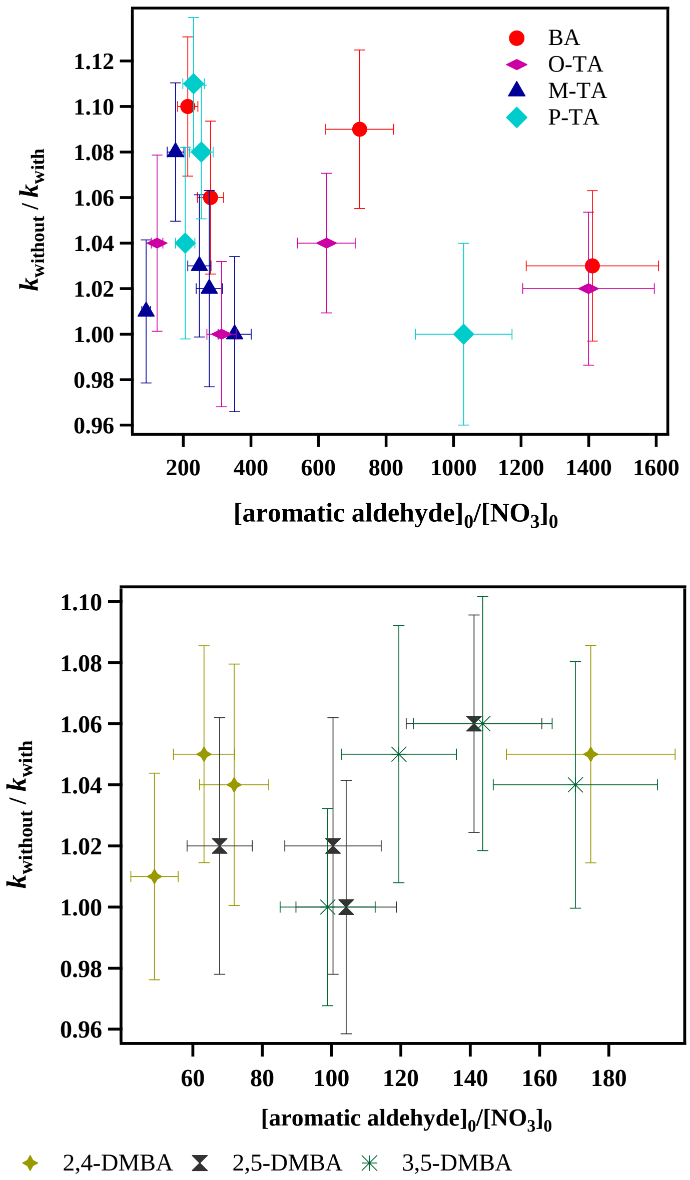

Figure S8 The ratio of rate coefficients without accounting for secondary reactions to that accounting for secondary reactions (using the reactions in Table S4) versus the ratio of initial aromatic aldehyde and NO$_3$ concentrations.

Table S1. List of specific masses monitored to detect various aromatic aldehydes using the PTR-TOF-MS and detection sensitivities and FTIR with the spectra range.

Aromatic aldehydes	PTR-TOF-MS		FTIR
	Mass charge ratio.H$^+$ (m/z)	detection sensitivity+2SD[a] (ncps/ppbv)	wavenumber (cm^{-1})
benzaldehyde	107.049	96.51±3.53	2760-2660
ortho-tolualdehyde	121.065	96.81±2.17	2780-2660
meta-tolualdehyde	121.065	128.76±3.42	2780-2660
para-tolualdehyde	121.065	135.02±1.78	2780-2660
2,4-dimethyl benzaldehyde	135.081	84.97±2.54	2780-2660
2,5-dimethyl benzaldehyde	135.081	79.19±2.47	2780-2660
3,5-dimethyl benzaldehyde	135.081	89.34±2.21	2780-2660

[a] the uncertainty of detection sensitivity was calculated as 2 times of standard deviation of the linear fitting in Figure S1 and the R^2 ranged from 0.95-0.99.

Table S2. The experimental conditions and rate coefficients for the reactions of aromatic aldehydes with NO_3 radical by relative method using methyl methacrylate (MMA) as reference. Aromatic aldehyde includes benzaldehyde (BA), o-tolualdehyde (O-TA), m-tolualdehyde (M-TA), p-tolualdehyde (P-TA), 2,4-dimethyl benzaldehyde (2,4-DMBA), 2,5-dimethyl benzaldehyde (2,5-DMBA) and 3,5-dimethyl benzaldehyde (3,5-DMBA).

Aromatic aldehydes	[Aromatic aldehydes] (10^{12} molecule cm^{-3})	ref [a]	no of experiments	$\frac{k}{k_{ref}} \pm error$ [b]	$k_{RR} \pm 2\sigma$ ($\times 10^{-15}$ cm^3 molecule^{-1} s^{-1}) [c]
BA	3.3-24.6	MMA	3	0.93±0.07	2.8±0.4
O-TA	2.2-3.4	MMA	3	2.84±0.06	8.5±1.0
M-TA	1.0-24.6	MMA	3	1.70±0.07	5.1±0.6
P-TA	2.5-3.4	MMA	3	1.69±0.02	5.0±0.6
2,4-DMBA	2.0-2.5	MMA	3	5.22±0.06	15.5±1.8
2,5-DMBA	1.6-24.6	MMA	3	4.48±0.16	13.4±1.6
3,5-DMBA	0.9-1.7	MMA	3	2.14±0.03	6.4±0.8

[a] $k_{ref+NO3}$ as: $k_{(MMA)}=(2.98\pm0.35)\times10^{-15}$ (Zhou et al., 2017)

[b] The errors estimated as detailed above.

[c] the uncertainties for k include the precision of our measured values and the quoted uncertainties in the rate coeffiecnts of references by using Eq.S1 in quadrature.

Table S3 The experimental conditions and the expected rate coefficients for the reaction of benzaldehyde (BA), o-tolualdehyde (O-TA), m-tolualdehyde (M-TA), p-tolualdehyde (P-TA), 2,4-dimethyl benzaldehyde (2,4-DMBA), 2,5-dimethyl benzaldehyde (2,5-DMBA) and 3,5-dimethyl benzaldehyde (3,5-DMBA) with NO_3 radical by absolute method using CRDS and Box model.

VOC	Initial mixing ratio of reactants (molecule cm^{-3})				k ($\times 10^{-15}$ cm^3 $molecule^{-1}$ s^{-1})		
	$[VOC]_0$ ($\times 10^{12}$)	$[NO_3]_0$ ($\times 10^{9}$)	$[N_2O_5]_0$ ($\times 10^{10}$)	$[NO_2]_0$ ($\times 10^{11}$)	k_{aro1} [a]	k_{aro2} [b]	k_{AR} [c]
BA	9.1	6.4	8.5	3.1	2.2±0.1	2.1±0.1	
	8.6	11.9	9.3	2.0	2.7±0.1	2.5±0.1	
	5.4	19.1	12.2	1.8	3.3±0.1	3.1±0.1	
	4.9	22.8	18.1	2.3	2.3±0.1	2.1±0.1	
				Average [d]	2.4±0.3	2.3±0.3	2.3±0.4
O-TA	2.7	4.3	5.6	3.3	8.5±0.2	8.2±0.2	
	1.5	5.9	6.3	2.2	9.4±0.2	9.3±0.2	
	3.4	27.9	36.5	3.9	9.9±0.3	9.5±0.3	
	3.1	9.9	15.0	4.5	9.8±0.2	9.8±0.2	
				Average [d]	9.3±0.5	9.1±0.5	9.1±1.2
M-TA	0.7	8.2	11.1	3.2	5.0±0.1	4.9±0.1	
	0.9	3.6	2.5	1.9	5.4±0.1	5.3±0.1	
	1.3	4.6	8.8	4.6	4.4±0.1	4.3±0.1	
	4.7	26.4	45.6	3.5	4.5±0.1	4.2±0.1	
	4.2	12.0	22.4	3.8	5.1±0.1	5.1±0.1	
				Average [d]	4.8±0.4	4.7±0.4	4.7±0.6
P-TA	1.7	6.8	7.0	2.4	5.1±0.1	4.7±0.1	
	3.1	3.0	7.8	6.1	5.2±0.1	5.2±0.1	
	8.6	37.4	26.4	1.9	5.6±0.1	5.0±0.1	
	4.1	20.1	11.0	1.2	4.4±0.1	4.2±0.1	
				Average [d]	5.1±0.4	4.8±0.4	4.8±0.6
2,4-DMBA	0.5	3.0	3.4	2.7	16.9±0.5	16.1±0.5	
	0.2	3.4	3.6	2.6	17.6±0.5	17.4±0.5	
	1.4	22.2	21.6	2.8	15.1±0.4	14.4±0.4	
	1.2	16.3	18.9	3.5	12.9±0.4	12.4±0.4	
				Average [d]	15.1±0.7	14.6±0.7	14.6±2.0
2,5-DMBA	0.3	2.8	4.1	3.5	12.2±0.4	12.2±0.4	
	0.4	2.9	2.5	2.1	12.3±0.3	11.6±0.3	
	2.2	32.7	30.5	2.7	12.9±0.4	12.7±0.4	
	1.9	19.0	22.2	3.4	12.9±0.4	12.7±0.4	
				Average [d]	12.5±0.6	12.2±0.7	12.2±1.7
3,5-DMBA	0.3	3.0	2.6	2.1	6.6±0.2	6.6±0.2	
	0.4	2.3	2.1	2.2	6.6±0.2	6.4±0.2	
	3.9	27.4	18.2	1.9	6.8±0.2	6.4±0.2	
	3.6	30.1	26.3	2.0	5.3±0.2	5.1±0.2	
				Average [d]	6.3±0.5	6.1±0.4	6.1±0.8

[a] The calculated values do not account for the secondary reactions listed in Table S4. Quoted errors are at the 95% confidence level based on the precision of the fitting.

[b] The calculated values include the contributions of the secondary reactions listed in Table S4. Quoted errors are at the 95% confidence level based on the precision of the fitting.

[c] The quoted errors include estimated systematic errors and the Student t-distribution contribution due to a limited number of measurements.

[d] Weighted average and error of repeated sampling was calculated using Eq.S2 and Eq.S3.

Table S4. Reaction scheme for NO_3 reacting with aromatic aldehydes in the presence of O_2 and nitrogen oxides that were included in simulating the temporal profiles of NO_3 and N_2O_5, and the yield of BAPAN.

Reactions	Rate coefficients 298 K, 1 bar air ($cm^3\ molecule^{-1}s^{-1}$ or s^{-1})	Reference
aromatic aldehydes $+NO_3 \xrightarrow{k_x} PhCOO_2 + HNO_3$	k_x (k_1-k_7)	this work
$NO_3+NO_2 \xrightarrow{k_9} N_2O_5$	1.35×10^{-12}	a
$N_2O_5 \xrightarrow{k_{10}} NO_3+NO_2$	0.04169	a
$NO_3 \xrightarrow{k_{11}}$ loss	k_{10}	b
$N_2O_5 \xrightarrow{k_{12}}$ loss	K_{11}	b
$PhCOO_2 + NO_2 \xrightarrow{k_{13}} PhCOO_2NO_2$	1.10×10^{-11}	c
$PhCOO_2NO_2 \xrightarrow{k_{14}} PhCOO_2 + NO_2$	3.18×10^{-4}	c
$PhCOO_2 + NO_3 \xrightarrow{k_{15}} PhCOO + NO_2 + O_2$		
Dialog to CH_3COO_2	3.20×10^{-12}	d
$PhCOO_2 + PhCOO_2 \xrightarrow{k_{16}} 2PhCOO+O_2$	1.5×10^{-11}	e
$PhCOO \xrightarrow{k_{17}} Ph+CO_2$		
Dialog to CH_3COO	1.0×10^{8}	f
$Ph+O_2 \xrightarrow{k_{18}} PhO_2$	1.8×10^{-11}	g
$PhO_2+PhO_2 \xrightarrow{k_{19}} 2PhO$	5.0×10^{-12}	e
$PhO_2+PhCOO_2 \xrightarrow{k_{20}} PhO + PhCOO$	1.0×10^{-11}	e
$PhO+PhO_2 \xrightarrow{k_{21}} Ph_2O$	5.0×10^{-12}	e
$PhO+PhO \xrightarrow{k_{22}} Ph_2O_2$	1.49×10^{-11}	h
$PhO+PhCOO_2 \xrightarrow{k_{23}} Ph_2CO+O_3$	2.0×10^{-11}	e
$Ph+Ph \xrightarrow{k_{24}} Ph_2$	1.91×10^{-11}	i

$PhO_2+NO_2 \xrightarrow{k_{25}} PhO_2NO_2$	1.1×10^{-11}	c
$PhO+NO_2 \xrightarrow{k_{26}} PhONO_2$	2.10×10^{-12}	c

[a] (J. B. Burkholder et al., 2015)

[b] (Derived from the first period of the experiments: observation in the absence of aromatic aldehyde)

[c] (Caralp et al., 1999)

[d] (Orlando and Tyndall, 2012)

[e] (Roth et al., 2010)

[f] (Hasson et al., 2012)

[g] (Yu and Lin, 1994)

[h] (Tao and Li, 1999)

[i] (Park and Lin, 1997)

Table S5. The initial concentration used in measuring the yield of BAPAN ($C_6H_5C(O)O_2NO_2$) in the reaction between benzaldehyde and NO_3.

Exp.	[benzaldehyde] $\times 10^{13}$ molecule cm^{-3}	$[NO_2]^a$ $\times 10^{13}$ molecule cm^{-3}	$[N_2O_5]$ $\times 10^{13}$ molecule cm^{-3}
1	1.4	~0	0.1
2	1.3	~0	1.5
3	1.3	~0	5.8
4	0.9	~0	6.3
5	1.0	2.5	5.6
6	1.1	2.8	13.7
7	1.1	13.5	14.7
8	1.0	32.5	12.2

[a] Shows additional NO_2 rather than the NO_2 was produced from N_2O_5 decomposition. In the main text, the value of NO_2 from the equilibrium between N_2O_5, NO_3, and NO_2 are added to these values to show the NO_2 concentration in the chamber.

Table S6. Net C-H bond dissociation enthalpies (BDEs) in aromatic aldehydes and the standard enthalpies of formation of the parent molecules and related radicals at 298.15 K and 0 K using Active Thermochemical Tables (ATcT) Thermochemical Network ver. 1.122x.[a]

Species name	Formula	BDE (kcal/mol)		$\Delta_f H^\circ$ (kcal/mol)	
		298.15 K	0 K	298.15 K	0 K
acetaldehyde	$CH_3C(O)$-H	89.28 ±0.06	87.86 ±0.06	-39.57 ±0.06	-37.05 ±0.06
acetyl	CH_3CO			-2.39 ±0.07	-0.82 ±0.07
benzaldehyde	$C_6H_5C(O)$-H	90.89 ±0.20	89.41 ±0.20	-8.98 ±0.19	-4.72 ±0.19
benzoyl	C_6H_5CO			29.81 ±0.26	33.05 ±0.26
ortho-tolualdehyde	o-$CH_3C_6H_4C(O)$-H	89.93 ±0.27	88.56 ±0.27	-15.99 ±0.26	-10.68 ±0.26
ortho-toluoyl	o-$CH_3C_6H_4CO$			21.84 ±0.34	26.24 ±0.34
meta-tolualdehyde	m-$CH_3C_6H_4C(O)$-H	90.85 ±0.27	89.35 ±0.27	-17.20 ±0.29	-11.73 ±0.29
meta-toluoyl	m-$CH_3C_6H_4CO$			21.54 ±0.34	25.99 ±0.34
para-tolualdehyde	p-$CH_3C_6H_4C(O)$-H	90.83 ±0.27	89.31 ±0.27	-17.42 ±0.28	-11.92 ±0.28
para-toluoyl	p-$CH_3C_6H_4CO$			21.32 ±0.34	25.76 ±0.34

[a] The quoted uncertainties are the best estimates of the corresponding 95% confidence intervals. The uncertainties for BDEs are obtained by using the full covariance matrix. Note that the enthalpies of formation of the radicals are highly correlated to those of the parent molecules, and thus the uncertainties of BDEs are smaller than those that would be obtained by propagating in quadrature the individual uncertainties of the relevant enthalpies of formation.

2. Correlation of the rate coefficients for reactions of NO_3 radical with those for the reactions of OH radicals

Canosa-Mas et al. (1988) showed a good correlation between the reactivities of alkynes towards OH and NO_3 radicals and attributed electrophilic addition in both cases. Sabljic and Gusten (1990) found a correlation between the rate coefficients of NO_3 and OH radicals reaction with 72 aliphatic compounds and benzene derivatives. Wayne et al. (1991) concluded that the general form of these correlations is a linear relationship between the logarithms of the rate coefficients for the reactions of NO_3 and those for the reactions of OH as a particular series of substrates:

$$\log(k_{NO3}) = a \times \log(k_{OH}) + b$$

In their review, Wayne et al. (1991) reviewed updated rate coefficients (Atkinson, 1997;Atkinson et al., 1997, 1999) for reaction with OH and NO_3 radicals. D'Anna et al. (2001) developed the correlation lines for abstraction and addition. The correlation line for H-atom abstraction from saturated hydrocarbons was given by:

$$\log(k_{NO3}) = (0.87 \pm 0.09) \times \log(k_{OH}) + (-6.0 \pm 1.0)$$

The correlation line for addition to unsaturated hydrocarbons is given by:

$$\log(k_{NO3}) = (3.43 \pm 0.24) \times \log(k_{OH}) + (22.7 \pm 2.5)$$

The correlation lines (green) for H-atom abstraction from the saturated hydrocarbons are shown in Figure S9. The addition pathways for NO3 and OH addition to olefins, aliphatic aldehydes, and the seven aromatic aldehydes obtained in this work are also shown in the figure. The correlation line (black) of 15 aliphatic aldehydes is given by:

$$\log(k_{NO3}) = (2.91 \pm 0.20) \times \log(k_{OH}) + (16.9 \pm 2.1);$$

The correlation line (red line) of 7 studied aromatic aldehydes is given by:

$$\log(k_{NO3}) = (1.56 \pm 0.38) \times \log(k_{OH}) + (2.44 \pm 4.08);$$

The correlation line (blue) of 15 aliphatic and 7 aromatic aldehydes together is given by:

$$\log(k_{NO3}) = (2.60 \pm 0.23) \times \log(k_{OH}) + (13.65 \pm 2.45).$$

Figure S9 shows that the aromatic aldehydes fall close to the line for the addition line, suggesting that the OH and NO_3 reaction with aromatic aldehydes also proceed through an addition pathway.

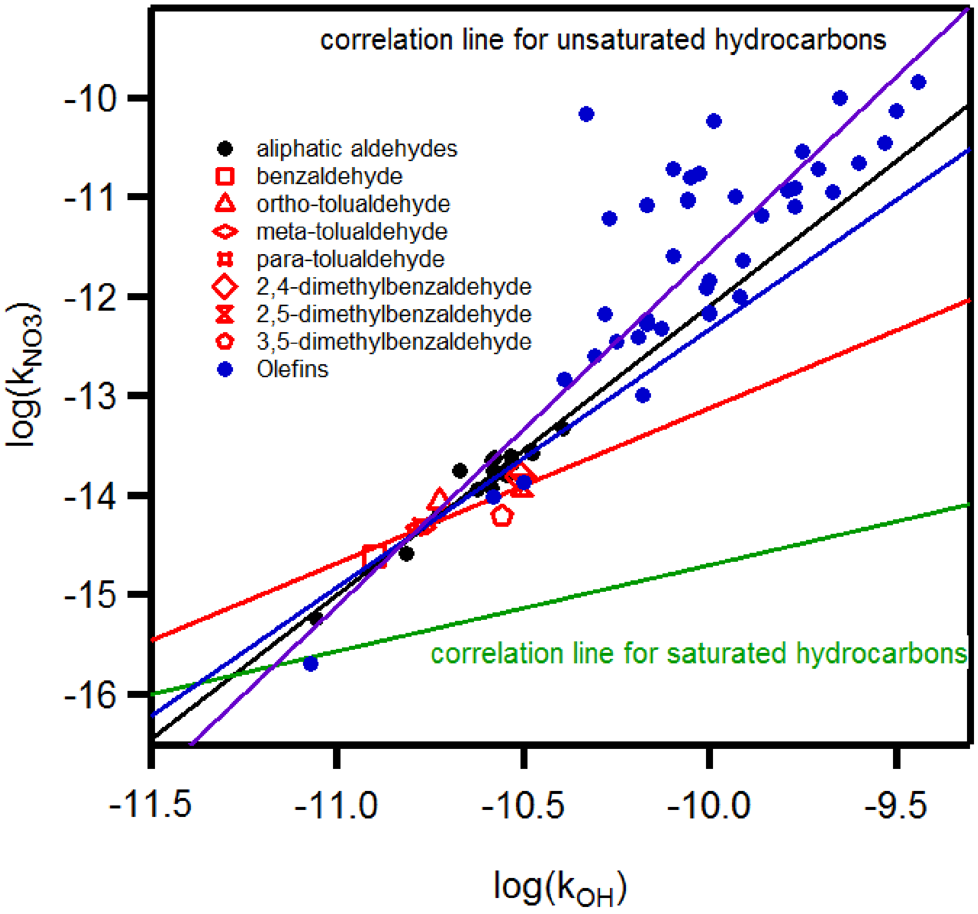

Figure S9 Linear free energy plot for the reactions of OH and NO_3 radicals with a series of 15 aliphatic aldehydes, 7 aromatic aldehydes and 41 olefins. The correlation line (green line) for H-atom abstraction of saturated hydrocarbons is given by: $\log(k_{NO3}) = (0.87 \pm 0.09) \times \log(k_{OH}) + (-6.0 \pm 1.0)$ and the correlation line (black line) of 15 aliphatic aldehydes is given by: $\log(k_{NO3}) = (2.91 \pm 0.20) \times \log(k_{OH}) + (16.9 \pm 2.1)$; the correlation line (red line) of 7 studied aromatic aldehydes is given by: $\log(k_{NO3}) = (1.56 \pm 0.38) \times \log(k_{OH}) + (2.44 \pm 4.08)$; the correlation line (blue line) of 15 aliphatic and 7 aromatic aldehydes is given by: $\log(k_{NO3}) = (2.60 \pm 0.23) \times \log(k_{OH}) + (13.7 \pm 2.5)$; the correlation line (violet line) of 15 aliphatic aldehydes, 7 aromatic aldehydes and 41 olefins is given by: $\log(k_{NO3}) = (3.54 \pm 0.19) \times \log(k_{OH}) + (23.9 \pm 1.9)$.

References

Atkinson, R.: Gas-Phase Tropospheric Chemistry of Volatile Organic Compounds: 1. Alkanes and Alkenes, J. Phys. Chem. Ref. Data, 26, 215-290, doi:http://dx.doi.org/10.1063/1.556012, 1997.

Atkinson, R., Baulch, D. L., Cox, R. A., Hampson, R. F., Kerr, J. A., Rossi, M. J., and Troe, J.: Evaluated Kinetic and Photochemical Data for Atmospheric Chemistry: Supplement VI. IUPAC Subcommittee on Gas Kinetic Data Evaluation for Atmospheric Chemistry, J. Phys. Chem. Ref. Data, 26, 1329-1499, doi:http://dx.doi.org/10.1063/1.556010, 1997.

Atkinson, R., Baulch, D. L., Cox, R. A., Hampson, R. F., Kerr, J. A., Rossi, M. J., and Troe, J.: Evaluated Kinetic and Photochemical Data for Atmospheric Chemistry, Organic Species: Supplement VII, J. Phys. Chem. Ref. Data, 28, 191-393, doi:http://dx.doi.org/10.1063/1.556048, 1999.

Canosa-Mas, C., Smith, S. J., Toby, S., and Wayne, R. P.: Reactivity of the nitrate radical towards alkynes and some other molecules, J. Chem. Soc., Faraday Trans. 2,, 84, 247-262, 10.1039/F29888400247, 1988.

Caralp, F., Foucher, V., Lesclaux, R., J. Wallington, T., and D. Hurley, M.: Atmospheric chemistry of benzaldehyde: UV absorption spectrum and reaction kinetics and mechanisms of the $C_6H_5C(O)O_2$ radical, Physical Chemistry Chemical Physics, 1, 3509-3517, 10.1039/A903088C, 1999.

D'Anna, B., Andresen, O., Gefen, Z., and Nielsen, C. J.: Kinetic study of OH and NO_3 radical reactions with 14 aliphatic aldehydes, Phys. Chem. Chem. Phys., 3, 3057-3063, 10.1039/B103623H, 2001.

Hasson, A. S., Tyndall, G. S., Orlando, J. J., Singh, S., Hernandez, S. Q., Campbell, S., and Ibarra, Y.: Branching Ratios for the Reaction of Selected Carbonyl-Containing Peroxy Radicals with Hydroperoxy Radicals, The Journal of Physical Chemistry A, 116, 6264-6281, 10.1021/jp211799c, 2012.

J. B. Burkholder, S. P. Sander, J. Abbatt, J. R. Barker, R. E. Huie, C. E. Kolb, M. J. Kurylo, V. L. Orkin, D. M. Wilmouth, and Wine, P. H.: Chemical Kinetics and Photochemical Data for Use in Atmospheric Studies, Evaluation No. 18, in, edited by: JPL Publication 15-10, J. P. L., Pasadena,, 2015.

Orlando, J. J., and Tyndall, G. S.: Laboratory studies of organic peroxy radical chemistry: an overview with emphasis on recent issues of atmospheric significance, Chemical Society Reviews, 41, 6294-6317, 10.1039/C2CS35166H, 2012.

Park, J., and Lin, M. C.: Kinetics for the Recombination of Phenyl Radicals, The Journal of Physical Chemistry A, 101, 14-18, 10.1021/jp961569i, 1997.

Roth, E., Chakir, A., and Ferhati, A.: Study of a Benzoylperoxy Radical in the Gas Phase: Ultraviolet Spectrum and C6H5C(O)O2 + HO2 Reaction between 295 and 357 K, The Journal of Physical Chemistry A, 114, 10367-10379, 10.1021/jp1021467, 2010.

Sabljic, A., and Gusten, H.: PREDICTING THE NIGHTTIME NO3 RADICAL REACTIVITY IN THE TROPOSPHERE, Atmos. Environ., 24, 73-78, 10.1016/0960-1686(90)90442-p, 1990.

Tao, Z., and Li, Z.: A kinetics study on reactions of C6H5O with C6H5O and O3 at 298 k, International Journal of Chemical Kinetics, 31, 65-72, 10.1002/(sici)1097-4601(1999)31:1<65::aid-kin8>3.0.co;2-j, 1999.

Wayne, R. P., Barnes, I., Biggs, P., Burrows, J. P., Canosamas, C. E., Hjorth, J., Lebras, G., Moortgat, G. K., Perner, D., Poulet, G., Restelli, G., and Sidebottom, H.: The nitrate radical - Physics, Chemistry, and the Atmosphere, Atmospheric Environment Part a-General Topics, 25, 1-203, 10.1016/0960-1686(91)90192-a, 1991.

Yu, T., and Lin, M. C.: Kinetics of the C6H5 + O2 Reaction at Low Temperatures, Journal of the American Chemical Society, 116, 9571-9576, 10.1021/ja00100a022, 1994.

Zhou, L., Ravishankara, A. R., Brown, S. S., Idir, M., Zarzana, K. J., Daële, V., and Mellouki, A.: Kinetics of the Reactions of NO_3 Radical with Methacrylate Esters, The Journal of Physical Chemistry A, 121, 4464-4474, 10.1021/acs.jpca.7b02332, 2017.